Broadband material characterization method using a CPW with a novel calibration technique

Broad-band Material Characterization Method Using a CPW with Novel Calibration Technique

L.A. Bronckers and A.B. Smolders, *Senior Member, IEEE*

***Abstract*—When combining contactless power and data transfer, antennas are often placed near magnetic materials with unknown RF properties. While permittivity measurement methods for dielectric materials at RF frequencies are well established, methods for permeability measurement are relatively scarce and often cumbersome. We propose a versatile and easy-to-use method that is applicable to both dielectric and magnetic materials, which uses a coplanar waveguide (CPW) structure to measure the complex permittivity and permeability in the 1-16 GHz range. We combine the Nicolson-Ross-Weir (NRW) algorithm with a robust root selection and a conformal mapping method to extract the permittivity and permeability from the measurement data. Moreover, we propose a novel calibration method that uses a single reference dielectric to increase the accuracy of the measured permittivity significantly, even when measuring magnetic materials.**

***Index Terms*—CPW, material characterization, NRW, permeability measurement, permittivity measurement**

I. Introduction

As devices become ever more integrated, contactless power and data transfer are often combined in a limited form factor. Often, magnetic materials (e.g. ferrites) are utilized to facilitate efficient magnetic power transfer. However, this poses a problem to the antenna design of the wireless data link, as the constitutional parameters of ferrites designed for power applications are often unknown at RF frequencies. Thus, the need for an easily applicable and versatile, yet sufficiently accurate, material characterization method for magnetic materials arises. While broad-band methods for material characterization at frequencies above 1 GHz are relatively well established for dielectric materials, convenient methods for characterization of magnetic materials are much rarer and often cumbersome.

In this letter, we propose a novel calibration technique that uses a single dielectric material with known properties to increase the accuracy of permittivity determination. Contrary to e.g. [1], this method can be used for both dielectric and magnetic materials and uses a reference material in addition to air to correct for the (unknown) air gap. Our setup uses a coplanar waveguide (CPW) transmission-line structure to obtain broad-band S-parameter measurements. We combine our calibration method with the Nicholson-Ross-Weir (NRW) algorithm and the well-known conformal mapping technique to extract the (complex) permittivity $\varepsilon_r = \varepsilon_r' - j\varepsilon_r''$ and permeability $\mu_r = \mu_r' - j\mu_r''$ of the material under test (MUT) from the measured S-parameters. Using our method, we obtain a very versatile and easily applicable setup that provides a reasonable accuracy.

First, the proposed system is described in section II, where the hardware and procedure are described in section II-A and the calculations are described in sections II-B and II-C. Next, the results are shown and discussed in section III. Finally, conclusions are drawn in section IV.

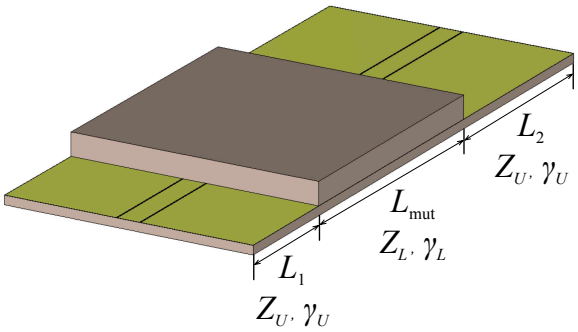

Fig. 1. 3D-view of the CPW with a MUT of length L_{mut} at distance L_1 from reference plane 1, and distance L_2 from reference plane 2. Only the CPW section between the calibration reference planes is shown.

II. Proposed System

While some resonator-based methods work over a large frequency range, e.g. [2], they can measure at only a limited number of frequency points, often followed by a curve-fitting procedure. Instead, in order to obtain a broad-band measurement, we use the non-resonant approach, where the MUT is introduced in a transmission line geometry, which is connected to a vector network analyzer (VNA). A schematic overview is given in Fig. 1, and the sections with and without a MUT in the geometry are referred to as loaded and unloaded, respectively. The material characteristics are calculated from the impedance Z_L and propagation constant $\gamma_{\text{L}} = \alpha_{\text{L}} + j\beta_{\text{L}}$ of the loaded section by applying the NRW algorithm [3], [4].

A. Measurement Hardware and Procedure

In order to facilitate a broad range of sample sizes, convenience of use and mitigate air gaps due to production/machining accuracy, we use a planar transmission line structure. For sensitivity considerations, a CPW without conductor backing is chosen. Instead of a conductor backing, we place the CPW on a material with properties close to that of vacuum (Rohacell 31HF [5]). A 3D view of the configuration is shown in Fig. 1, where a MUT is placed on the CPW. A cross-sectional view of the loaded section with indicated material properties and dimensions is shown in Fig. 2.

We have designed the unloaded CPW for a 50Ω impedance to facilitate accurate calibration, and to minimize reflections from the measurement system. To maximize the sensitivity to the MUT we want the fields to extend as far above the

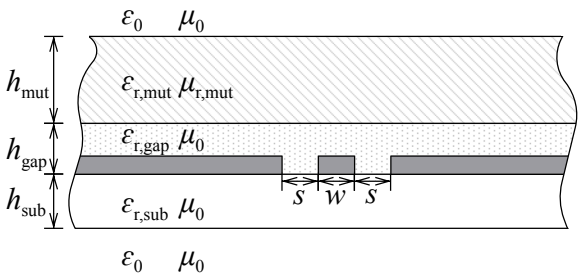

Fig. 2. Cross-sectional view of the assumed configuration for the conformal mapping method. All relevant heights and parameters are indicated. Note that the metallization height is included in the gap layer.

TABLE I
PROPERTIES OF THE MUT SAMPLES

Material	ε_r	μ_r	$L_{\mathbf{mut}}$	$h_{\mathbf{mut}}$
TMM10i [9]	9.80 - j0.02	1	30 mm	1.92 mm
TP20419 [10]	2.75 - j0.001	1	30 mm	2.96 mm
FGM125 [11]	7	3.5-j2 @ 1 GHz	10 mm	3.25 mm

CPW as possible. Therefore we select a substrate with low permittivity (Rogers RT/duroid 5880, $\varepsilon_r = 2.20$ [6]), which has metallization thickness $h_m = 17\,\mu m$ and substrate thickness $h_{sub} = 787\,\mu m$, which is sufficiently thick for mechanical stability, but thin enough to ensure operation below the cutoff frequency of the TE_0 mode in the frequency range of interest [7]. A thin (0.5 to $1\,\mu m$) coating (OSP-Glicoat SMD F2(LX)) is applied to avoid corrosion, but we apply no solder mask or silk screen. We choose center conductor width $w = 2$ mm, which results in gap width $s = 89\,\mu m$, and use SMA end launch connectors with a conductor-backed CPW launch area to connect the VNA to the board. In order to shift the reference planes to the desired locations, such that only a 50 mm CPW is left between the reference planes, we apply a TRL calibration [8] with the required standards fabricated on the PCB. The final measurement setup, with a 30 mm long sample, is shown in Fig. 3.

Since the MUT is positioned by hand using a digital caliper, positioning errors will occur. Therefore, we repeat the complete measurement 5 to 10 times for each sample. We then discard outliers and choose the measurement that best represents the average of the remaining measurements as the final result. The minimum and maximum of the remaining measurements will be indicated at regular intervals using error bars. We tested the setup by measuring samples with known characteristics: Rogers TMM10i, Premix Preperm TP20419 and Eccosorb FGM125. Their electromagnetic properties are summarized in Table I. We have also performed a numerical error analysis, in which random perturbations are added to calculated (ideal situation) S-parameters. This shows that, for high loss materials, the error sensitivity decreases with decreasing L_{mut}, up to a certain point from which the sensitivity increases again. While a long sample results in decreased error sensitivity for low-loss materials, it causes high losses in lossy materials, decreasing the power that the VNA receives and thus increasing the error sensitivity Therefore, for low-loss

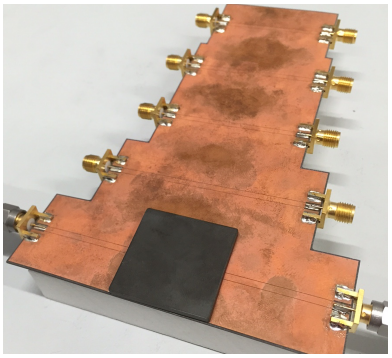

Fig. 3. Complete measurement setup. The board is placed on Rohacell 31HF, and during the actual measurement the MUT is clamped tightly to the board.

materials we use L_{mut} = 30 mm, while we choose a shorter sample length L_{mut} = 10 mm for lossy materials.

B. Algorithm

The calculations consist of three stages. First, we de-embed the unloaded sections (L_1 and L_2) by shifting the reference planes, assuming a homogeneous cross-section, which is done using the measured propagation constant of the unloaded line. We then use the NRW algorithm to extract the effective constitutional parameters of the loaded section, denoted as $\varepsilon_{r,eff}$ and $\mu_{r,eff}$, again assuming a homogeneous cross-section. Finally, the MUT constitutional parameters are extracted from the effective constitutional parameters of the homogeneous loaded section using a conformal mapping method.

The NRW algorithm involves taking the logarithm of a complex number, which results in an infinite number of roots. This was originally solved by Weir [4] by comparing measured and calculated group delays. Another method for the root selection, based on a Kramers-Krönig relationship between α and β in the propagation constant $\gamma = \alpha + j\beta$, was proposed by Varadan et al. [12]. In addition, a method based on phase-unwrapping has been proposed [13], but the determination of the initial phase was based on the assumption of a low-loss dispersion-free material. In this study, we use a new combination of existing methods for root selection. The initial root is determined at low frequencies by group delay comparison, as a basis for performing phase-unwrapping for higher frequencies. This method solves the initial root problem [13], and is more robust than other methods.

C. Gap Calibration

The cross-section used for the conformal mapping method is shown in Fig. 2. We propose a new method to calibrate errors in the configuration out of the measurement: in addition to the substrate and MUT, we introduce an additional layer (referred to as gap layer) between the substrate and the MUT. We refer to this method to as "gap calibration", and the correction itself as "gap correction". Since these effects cannot be separated, the gap layer includes all, previously unaccounted for, effects near the metallization: the air gap between sample and metallization, surface roughness, metallization thickness, imperfections in metallization and substrate, and the glicoat

surface finish (which has unknown characteristics). The gap calibration consists of determining the gap height and permittivity by measuring a MUT with known characteristics and the empty line. Thus, only a single reference sample is required, giving two reference points to calculate the gap height and permittivity. The gap height and permittivity are then found iteratively using a Levenberg-Marquardt (LM) algorithm at each frequency point, assuming a relative permeability equal to 1. In order to calibrate as much of the systematic errors out as possible, the gap height and permittivity are allowed to be frequency dependent. After the calibration, the determined gap height and permittivity are used to correct the calculations for other materials. We use the Rogers TMM10i sample as the reference material, assuming that this material is dispersion-free in the tested frequency range.

We can express the MUT permittivity in terms of the gap properties, effective permittivity and filling factors as [14]:

$$\varepsilon_{\mathrm{r,mut}} = \frac{\varepsilon_{\mathrm{r,eff}} - 1 - q_1 - q_2\varepsilon_{\mathrm{r,gap}} - q_3(\varepsilon_{\mathrm{r,sub}} - 1)}{q_1 - q_2}, \quad (1)$$

where q_1, q_2 and q_3 are filling factors as defined in [14] ($h_1 = h_{\mathrm{mut}} + h_{\mathrm{gap}}$, $h_2 = h_{\mathrm{gap}}$, $h_3 = h_{\mathrm{sub}}$), $\varepsilon_{\mathrm{r,eff}}$ is the effective relative permittivity of the cross-section, and $\varepsilon_{\mathrm{r,mut}}$, $\varepsilon_{\mathrm{r,sub}}$ and $\varepsilon_{\mathrm{r,gap}}$ are the relative permittivity of MUT, substrate and gap, respectively.

The duality between permittivity and permeability introduced by Pucel [15] for conformal mapping of microstrip lines on magnetic substrates can also be applied to a CPW configuration [16]. Assuming that the MUT is the only material with non-unity relative permeability, we can apply Pucel's duality to Equation 1 to calculate the MUT permeability from the effective permeability:

$$\mu_{\mathrm{r,mut}} = \frac{q_1 - q_2}{\frac{1}{\mu_{\mathrm{r,eff}}} - 1 + q_1 - q_2}. \quad (2)$$

The gap height h_{gap} is set to 0 for the determination of the MUT permeability from the effective permeability. Thus, the CM method for permeability reduces to the more conventional one without a gap layer, and the gap correction is not applied to the permeability calculation. This is done since we do not have materials with accurately known $\mu_{\mathrm{r,mut}} \neq 1$ available to obtain a reference value.

III. Results

A comparison of the measured permittivity of the 30 mm Premix material with and without gap correction is shown in Fig. 4a, and a comparison of the relative error of the real permittivity is shown in Fig. 4b. Due to a high reflection from the SMA to CPW transition, no calibration can be performed in the frequency range around 5.8 GHz. Therefore, no results are shown in that range. It is clear that the gap correction improves the accuracy of the real part of the permittivity: without gap correction, the relative error is around 10% below 5 GHz, while it is less than 2% up to 5 GHz when the gap correction is applied. Apart from an inaccuracy peak where a dimensional resonance occurs in the sample, the accuracy of the real part of the permittivity is better than 5% up to 16 GHz when the gap correction is applied. The imaginary part

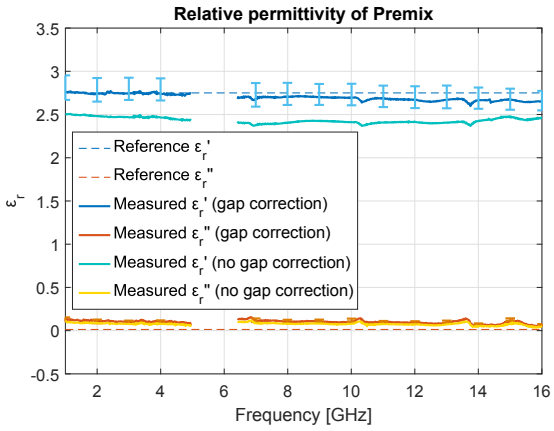

(a)

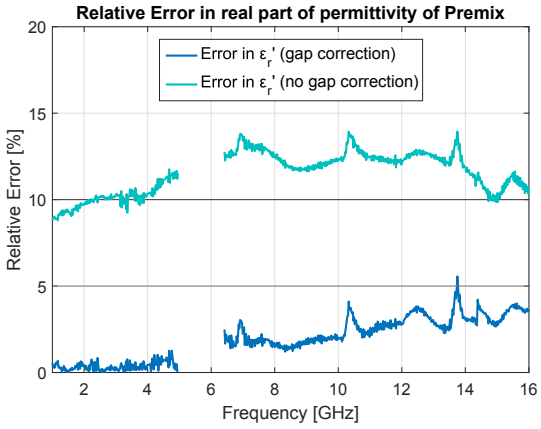

(b)

Fig. 4. Measured permittivity (a) and relative error in real part of permittivity (b) of TP20419. The minimum and maximum of the measured values are indicated by error bars. Reference data obtained from [10], assuming no dispersion in the measured frequency range.

of the permittivity (Fig. 4a), while over-estimated, is almost unaffected by the gap calibration.

Fig. 5 shows the permittivity measurement of a 10 mm FGM125 sample, where the permittivity with and without gap correction are compared in Fig. 5a, and the relative error in the real part of the relative permittivity in Fig. 5b. Since the gap correction is not applied to the permeability, the permeability results with and without gap correction are the same and shown in Fig. 5c. The ripple with approximately 2 GHz peak-to-peak spacing is due to the high reflection from the SMA launch area, which causes an instability in the NRW algorithm when the permeability is not fixed. It is clear that the measurement does not work well at high frequencies ($>$ 14 GHz) for this material, as the quasi-TEM assumption is violated for high frequencies. Without the gap calibration, the obtained permittivity is, like the premix material, too low. Applying the gap calibration, the measured relative permittivity is within 10% of the value specified by the manufacturer up to 5 GHz. Hyde [17], [18] also found a slightly higher value for the real permittivity, using various methods. Again, the imaginary part of the permittivity is over-estimated, but hardly affected by the gap calibration. The real permeability matches very well,

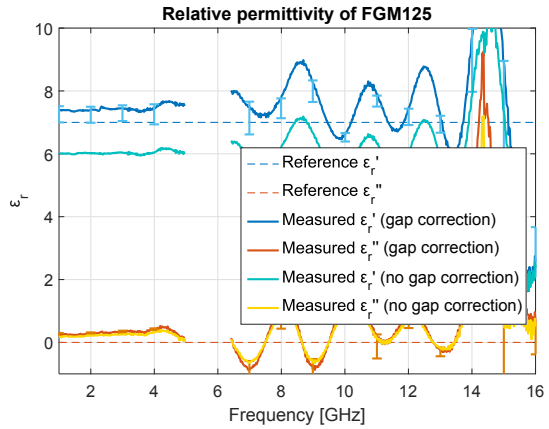

(a)

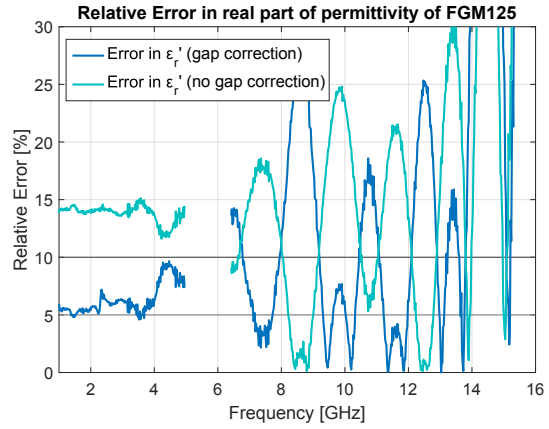

(b)

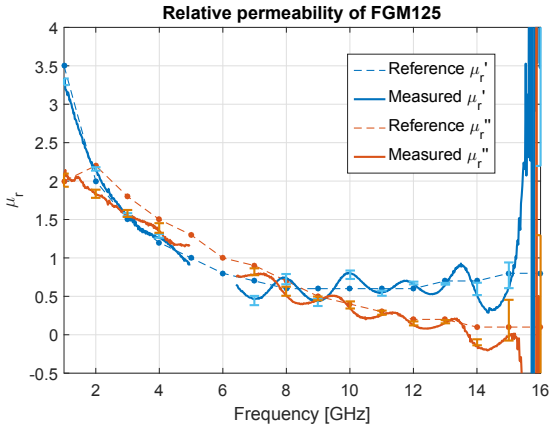

(c)

Fig. 5. Measured permittivity (a), relative error in real part of permittivity (b) and permeability (c) of FGM125. The minimum and maximum of the measured values are indicated by error bars. Reference data obtained from [11].

even for $\mu_r' < 1$, while the match of the imaginary part of the permeability is less good. However, as the measured imaginary part of the permeability does not exhibit the peak specified by the manufacturer at 2 GHz and otherwise provides a good match, it seems likely that the deviation is due to process variation in the material fabrication or possibly a measurement error by the manufacturer.

IV. Conclusion

We present a versatile and very broad-band material characterization method that is able to characterize both dielectric and magnetic materials. In principle, the method can be used up to any frequency, and could be extended to frequencies above 16 GHz by adapting the measurement hardware or using a full-wave model. Samples can be easily fabricated, and the measurement hardware is relatively cheap to produce. We successfully combine the NRW method, using a novel robust method for root selection, with conformal mapping to extract the MUT's constitutional parameters from the measurement data. Moreover, we have developed a new calibration method that uses air and a known dielectric as references to improve the accuracy of permittivity measurements, even for magnetic materials.

Acknowledgment

The authors would like to thank TE Connectivity Den Bosch, The Netherlands, in particular Dirk-Jan Riezebos, Gied Habraken and Wijnand van Gils, for their support of this work.

References

[1] N. K. Das, S. M. Voda, and D. M. Pozar, "Two methods for the measurement of substrate dielectric constant," *IEEE Trans. Microw. Theory Techn.*, vol. 35, no. 7, pp. 636–642, Jul. 1987.
[2] *Substrate Measurement System (SMS)*, AixaTech GmbH, 2010.
[3] A. Nicolson and G. Ross, "Measurement of the intrinsic properties of materials by time-domain techniques," *IEEE Trans. Instrum. Meas.*, vol. 19, no. 4, pp. 377–382, Nov. 1970.
[4] W. B. Weir, "Automatic measurement of complex dielectric constant and permeability at microwave frequencies," *Proc. IEEE*, vol. 62, no. 1, pp. 33–36, Jan. 1974.
[5] *Dielectric Properties Rohacell HF*, Evonik Industries, May 2011.
[6] *RT/duroid 5870/5880 High Frequency Laminates*, Publication #92-101, Rogers, 2014.
[7] K. Gupta, R. Garg, I. Bahl, and P. Bhartia, *Microstrip Lines and Slotlines*. Norwood, MA: Artech House, 1996.
[8] *Network Analysis Applying the 8510 TRL Calibration for Non-Coaxial Measurements, Technical Overview*, 5091-3645E, Keysight Technologies, Jul. 2014.
[9] *TMM Thermoset Microwave Materials*, Publication #92-108, Rogers, 2013.
[10] *Premix Preperm TP20419, Preliminary Technical Datasheet*, Premix Group, Apr. 2014.
[11] *Eccosorb FGM: Permittivity & Permeability Data*, Emerson & Cuming Microwave Products, Aug. 2007.
[12] V. V. Varadan and R. Ro, "Unique retrieval of complex permittivity and permeability of dispersice materials from reflection and transmitted fields by enforcing causality," *IEEE Trans. Microw. Theory Techn.*, vol. 55, no. 10, pp. 2224–2230, Oct. 2007.
[13] L. Chen, T. M. Grzeqorczyk, B.-I. Wu, J. Pacheco Jr., and J. A. Kong, *Microwave Electronics: Measurement and Materials Characterization*. Chichester, England: John Wiley & Sons Ltd., 2004.
[14] E. Carlsson and S. Gevorgian, "Conformal mapping of the field and charge distributions in multilayered substrate CPW's," *IEEE Trans. Microw. Theory Techn.*, vol. 47, no. 8, pp. 1544–1552, Aug. 1999.
[15] R. A. Pucel and D. J. Massé, "Microstrip propagation on magnetic substrates - part I: Design theory," *IEEE Trans. Microw. Theory Techn.*, vol. 20, no. 5, pp. 304–308, May 1972.
[16] J. Hinojosa, "Coplanar propagation on magnetic substrates," *Microwave and Optical Technology Letters*, vol. 31, no. 5, pp. 365–368, Dec. 2001.
[17] M. W. Hyde IV and M. J. Havrilla, "Measurement of complex permittivity and permeability using two flanged rectangular waveguides," in *Microwave Symposiom, 2007. IEEE/MTT-S International*, 2007, pp. 531–524.
[18] M. W. Hyde IV, M. J. Havrilla, A. E. Bogle, and N. J. Lehman, "Broadband characterization of materials using a dual-ridged waveguide," *IEEE Trans. Instrum. Meas.*, vol. 62, no. 12, pp. 3168–3176, Dec. 2013.